Remote sensing variables as predictors of habitat suitability of the viscacha rat (Octomys mimax), a rock-dwelling mammal living in a desert environment

Valeria E. Campos, Gabriel Gatica & Laura M. Bellis

Volume 60 · Number 2 · April 2015

60th Anniversary

Mammal Research

Springer

Mammal Research Institute
Polish Academy of Sciences
Białowieża

Springer

Springer

ORIGINAL PAPER

Remote sensing variables as predictors of habitat suitability of the viscacha rat (*Octomys mimax*), a rock-dwelling mammal living in a desert environment

Valeria E. Campos · Gabriel Gatica · Laura M. Bellis

Abstract Identifying high-quality habitats across large areas is a central goal in biodiversity conservation. Remotely sensed data provide the opportunity to study different habitat characteristics (e.g., landscape topography, soil, vegetation cover, climatic factors) that are difficult to identify at high spatial and temporal resolution on the basis of field studies. Our goal was to evaluate the applicability of remotely sensed information as a potential tool for modeling habitat suitability of the viscacha rat (*Octomys mimax*), a rock-dwelling species that lives in a desert ecosystem. We fitted models considering raw indices (i.e., green indices, Brightness Index (BI) and temperature) and their derived texture measures on locations used by and available for the viscacha rat. The habitat preferences identified in our models are consistent with results of field studies of landscape use by the viscacha rat. Rocky habitats were well differentiated by the second-order contrast of BI, instead of BI only, making an important contribution to the global model by capturing the heterogeneity of the substratum. Furthermore, rocky habitats are able to maintain more vegetation than much of the surrounding desert; hence, their availability might be estimated using SATVI (Soil Adjusted Total Vegetation Index) and its derived texture measures: second-order contrast and entropy. This is the first study that evaluates the usefulness of remotely sensed data for predicting and mapping habitat suitability for a small-bodied rock dwelling species in a desert environment. Our results may contribute to conservation efforts focused on these habitat specialist species by using good predictors of habitat quality.

Keywords Habitat selection · Soil Adjusted Total Vegetation Index · Image texture · Rocky habitat · Viscacha rat · Desert ecosystem

V. E. Campos
Interacciones Biológicas del Desierto (INTERBIODES),
IMCN - Universidad Nacional de San Juan, Av. Ignacio de la Roza 590 (Oeste), 5400, Rivadavia, San Juan, Argentina

V. E. Campos · G. Gatica
Departamento de Biología y Museo de Ciencias Naturales, Facultad Ciencias Exactas, Físicas y Naturales, Universidad Nacional de San Juan, San Juan, Argentina

V. E. Campos (✉) · G. Gatica · L. M. Bellis
Consejo Nacional de Investigaciones Científicas y Técnicas (CONICET), Buenos Aires, Argentina
e-mail: vcampos@unsj-cuim.edu.ar

L. M. Bellis
Instituto de Diversidad y Ecología Animal (IDEA) CONICET/UNC and Facultad de Ciencias Exactas Físicas y Naturales, Universidad Nacional de Córdoba, Córdoba, Argentina

Introduction

One of the main goals in biodiversity conservation and land-use planning is to identify and preserve important areas for wildlife. Species conservation usually focused on the most suitable habitat for a species of concern, but the challenge is to identify high-quality habitat across large areas (Bellis et al. 2008). A species' habitat is affected by environmental characteristics that vary in space and time; therefore, the habitat model needs continuous spatial measurements of biophysical predictors that are difficult to identify on the basis of field studies (Nagendra 2001; Bradley et al. 2012).

Remotely sensed data can provide information about landscape topography (Brown 1994), soil (Bolstad and Lillesand

1992), rainfall, and temperature (Austin et al. 1994), as well as about habitat attributes (Osborne et al. 2001) and vegetation cover (Pettorelli et al. 2005), factors that shape the distribution of species. These data can improve the overall accuracy of a habitat model for a target species (Bradley et al. 2012) because they provide information about habitat variables at high spatial and temporal resolution and can be quantified across broad extents (Nagendra 2001).

Many species distribution and habitat suitability models are based on land cover class abundance (Card 1982; Olofsson et al. 2013); however, the use of classified images relies on pre-defined ecological classes that aggregate different habitat types and are rarely based on real habitat requirements of specific wildlife species (Gottschalk et al. 2005). Categorical variables, such as land cover vegetation, may be poor predictors of the species-habitat relationship, because they cannot account for within-class variability (St-Louis et al. 2006); therefore, more informative proxy variables are established by developing continuous relationships between remote sensing data and important habitat features, such as vegetation structure (Turner et al. 2003; St-Louis et al. 2006; Bellis et al. 2008; Wood et al. 2012). In many studies, greenness indices have served as a proxy for vegetation productivity or biophysical parameters such as leaf area index, which have been extensively used as predictors of habitat characteristics for animals. Willems and Hill (2009) used NDVI (Normalized Difference Vegetation Index) to model habitat of the vervet monkey (*Chlorocebus pygerythrus*) in Africa. Some phenological metrics derived from NDVI time series has been correlated with mosquito life cycles in Africa (Rogers et al. 2002), habitat of great bustards (*Otis tarda*) in Spain (Osborne et al. 2001), and moose body mass (*Alces alces*) in Norway (Herfindal et al. 2006). In addition, spatial habitat heterogeneity can be evaluated through image-based measures, i.e., texture measures derived from satellite imagery. These indices allow us to quantify the heterogeneity within a defined area of an image as a continuous variable (St-Louis et al. 2006, 2009; Bellis et al. 2008; Wood et al. 2012, 2013). Texture measures have been used for characterizing vegetation patterns (Ge et al. 2006) and have been successfully applied in different species and environments to predict the occurrence of bird species in grassland (Bellis et al. 2008); desert ecosystem (St-Louis et al. 2006, 2009); grassland, savanna, and woodland (Wood et al. 2012) as well as the occurrence of large-sized mammals, such as the antelope (*Tragelaphus eurycerus isaaci*) in mountain forests in Kenya (Estes et al. 2008). NDVI texture, as opposed to NDVI only, captures heterogeneity in the amount of greenness, e.g., it accounted for 65 % of the variability in plant species richness in the Canadian Arctic (Gould 2000) and was the best predictor of bird species richness among all of the measures from individual Landsat TM bands in the Chihuahuan Desert, New Mexico (St-Louis et al. 2009).

The ability of remote sensing to detect important habitat features varies according to the characteristics of a species and its ecosystem (Turner et al. 2003). Although these variables are widely used to model animal habitat, habitat features other than vegetation are rarely evaluated. For habitat specialists, such as rock-dwelling mammals, rocky habitat is a limited resource for their distribution (Walker et al. 2003); hence, differentiating substrata through remote sensing data can be useful to identify suitable habitats. Rocky habitats are found in almost every ecosystem around the world, ranging from extremely hot, dry deserts to very cold alpine regions; these habitats can occur uninterruptedly across the landscape, e.g., continuous mountains, or be clumped and isolated, e.g., isolated boulder piles or small hills (Nutt 2007). Rock-dwelling rodents are able to survive in extreme environments because the complexity of rocky habitats provides shelter, nesting sites, and breeding sites in a thermally stable microclimate that is also relatively safe from predators and competitors. The insulating ability of rocks to moderate extreme fluctuations in ambient temperature helps many rock-dwelling species to properly thermoregulate (Nutt 2007). Moreover, the depressions in rocks form small water catchments during periods of rain, increasing humidity and favoring plant species richness, therefore leading to a mesic habitat (Nutt 2007), another important feature particularly in a desert environment.

Our goal here was to evaluate the applicability of remotely sensed data as a potential tool for modeling habitat suitability of the viscacha rat (*Octomys mimax*), a rock-dwelling species that lives in a desert ecosystem. This rodent is endemic to central-western Argentina and is a good species for assessing the capacity of remotely sensed prediction because it is a habitat specialist species that selects rocky crevices in outcrops (Ebensperger et al. 2008; Traba et al. 2010; Campos 2012; Campos and Giannoni 2013) with high cover vegetation compared with surrounding areas (Campos 2012). At microhabitat scale, it has been shown that the viscacha rat selected deep and narrow crevices that are thermally stable and might facilitate thermoregulation (Campos et al. 2013).

Here, we addressed the following questions: (1) which remote sensing predictors are best associated with viscacha rat occurrence? (2) How well do models with remotely sensed data predict the occurrence of this species? (3) What is the potential distribution of the viscacha rat in the study area?

Methods

Study area

The study was conducted in Ischigualasto Provincial Park (IPP; Fig. 1), San Juan province, Argentina (29° 55′ S, 68°
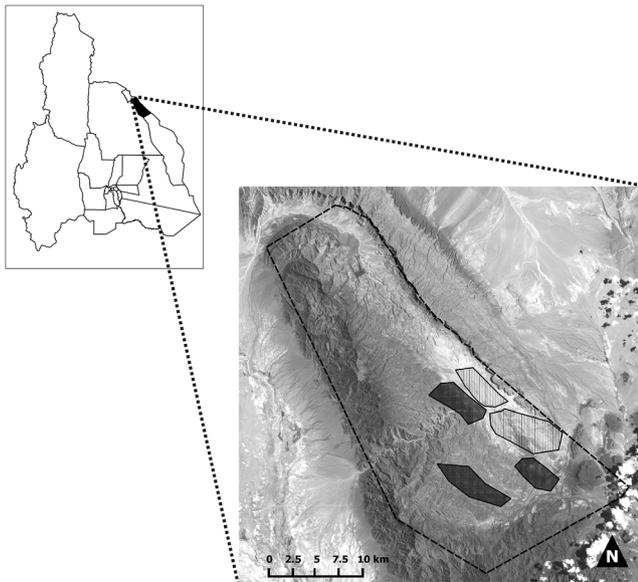
Fig. 1 Map of Ischigualasto Provincial Park (*dashed line*). The *polygons* indicate the sampling area with different substrata: 1—rocky areas with irregular topography and frequent fissures (*dotted polygons*); 2—areas with fine substrata, clay, and sandy soils (*barred polygons*)

05′ W). The Park has an area of 62,916 ha and is located in a hyper-arid sector of the Monte Desert, which corresponds to the northern Monte of hills and closed basins (Monte de Sierras y Bolsones). Average annual precipitation is 100 mm (Labraga and Villalba 2009). Temperature is characterized by considerable day/night variations and a wide range throughout the year, with absolute maximum and minimum values of 46.2 and 12.8 ° C, respectively, in summer and 39.4 and 9.9 ° C, respectively, in winter (Campos 2012). The study area is dominated by rocky outcrops of sandstones with varying salt content; moreover, there are areas of fine-textured substrata (sands and clays) where water accumulates after a rainfall event (Márquez et al. 2005). The vegetation is xerophytic due to the low rainfall and high temperatures, and is characterized by open scrublands dominated by shrubs (*Larrea cuneifolia*, *Zuccagnia punctata*, *Prosopis torquata*), cacti (*Echinopsis terscheckii*), and bromeliads, such as *Deuterocohnia longipetala*, and *Tillandsia* spp. (Márquez et al. 2005). Vegetation cover is heterogeneous, ranging from 5 to 80 % (Márquez et al. 2005).

Field survey

Fieldwork was conducted in the dry season (from May to August) of 2010 ($n=90$) and 2011 ($n=96$), because a previous study involving the same populations showed that a great number of crevices were used in this season (Campos and Giannoni 2013). During this period, when the food resource is scarce, the viscacha rat probably increases its foraging area and therefore may frequently move to and from occupied crevices. Another reason for the high use of crevices in the

dry season could be an increase in density by new births in the wet season and dispersal of young in the dry season.

We used a Landsat 5 TM image with 30-m resolution acquired on 8 February 2010 (path 232, row 081) stored in a geographic information system program (Quantum GIS Version 1.7.0 "Wroclaw"). We selected random field points ($N=186$) in areas with different substrata: 1—rocky areas with irregular topography and frequent fissures ($N=90$; Fig. 2a); 2—areas with a fine substratum of clay and sand ($N=96$; Fig. 2b). The total sampled area was of 12,583 ha, with field points separated by at least 100 m.

To evaluate selection, we applied a use–availability design (Boyce et al. 2002; Johnson et al. 2006) because accurate identification of unused points might be impractical or impossible (Johnson et al. 2006). We classified each field point as used or available based on signs of the presence of viscacha rat in a 900-m² area. Used locations were those that had crevices with signs, i.e., feces, caches of plant material, footprints, and loose soil. We considered available locations both those without crevices and those with crevices but that had no viscacha rat signs or had spider webs and leaf cover.

Remote sensing variables

Different indices were calculated using the Landsat image for the field survey. The spectral behavior of the substratum is influenced by different factors, such as chemical composition, texture, structure and moisture content (Labrandero 1978). The Tasseled Cap transformation (TC; Kauth and Thomas 1976; Crist and Cicone 1984) results in new bands by combining the originals bands of the image, in order to enhance some features of interest. The first Tasseled Cap index (Brightness Index, BI) provides data on soil signature, the second index (Greenness Index, GI) reflects vegetation characteristics, and the third index (Wetness Index, WI) captures information on the interaction of soil and vegetation. Previous studies have reported that BI is useful to determine substratum heterogeneity in a desert because it is a measure of reflectivity on the image (Martinelli 2009; Gatica 2010). Since BI provides information about reflectivity particularly generated by the soil, we used it to assess the type of substratum on locations used by and available to the viscacha rat.

Several satellite-derived vegetation indices, especially those obtained from the difference between near-infrared and visible red bands, such as NDVI, are estimators of green and vigorous vegetation, but showed limited success in measuring senescent and leafless vegetation (Goirán et al. 2012). Since in arid environments like the Monte Desert, vegetation has small leaf area and non-photosynthetic tissues for long periods and is distributed in patches scattered throughout a matrix of bare soil (Goirán et al. 2012), the most commonly used green index does not usually have a good fit. We evaluated green indices with a correction factor for soil background effects (Huete

Fig. 2 a Rocky areas with irregular topography and frequent fissures. **b** Areas with fine substrata, clay, and sandy soils
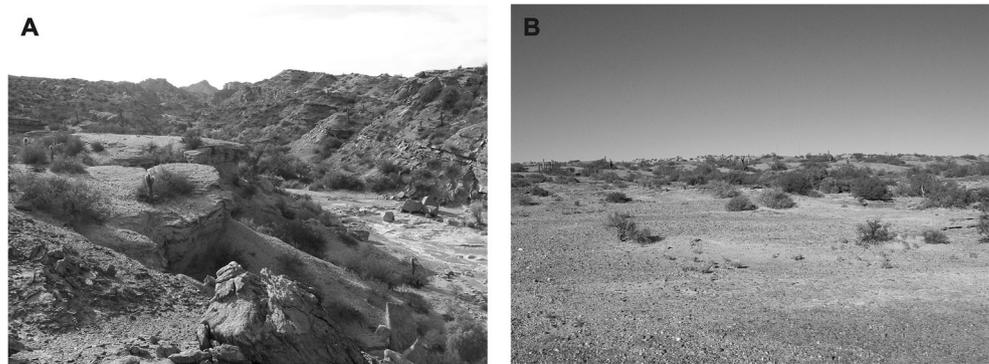
1988) and sensitive to both, green and senescent vegetation (Goirán et al. 2012). We tested raw greenness indices as independent variables in models: NDVI and GI from TC (Kauth and Thomas 1976; Crist and Cicone 1984) both sensitive to green vegetation, NDSVI (Normalized Difference Senescent Vegetation Index; Marsett et al. 2006), which quantifies senescent and green biomass, SAVI (Soil Adjusted Vegetation Index; Huete 1988), which is sensitive to green vegetation but includes a parameter that normalizes the effect of bare soil factor, and SATVI (Soil Adjusted Total Vegetation Index; Marsett et al. 2006), which is sensitive to both green and senescent vegetation, and includes a parameter that normalizes the effect of bare soil factor. In SAVI and SATVI, the parameter L has values of 1 for low vegetation cover, 0.5 for intermediate values, and 0.25 for high vegetation cover (Huete 1988). For PPI, we considered a value of 0.5 for the parameter L.

In the Landsat image 5 TM, the band 6 digital values represent the mean values of the radiance from the instantaneous field of view of the sensor, 120 m^2 on the ground, after atmospheric propagation. With the assumption of an emissivity equal to 1 and without considering any atmospheric effects, brightness temperatures can be calculated for each pixel using the equations of Schott and Volchok (1985).

Image texture is a remote sensing approach of spatial variability on gray level (i.e., gray shadow of pixels); hence, it contains important information about the spatial and structural arrangement of objects in an image (Haralick et al. 1973; Mihran and Jain 1998). First-order texture measures are based on the number of occurrences of each gray-level within a given processing window. Second-order texture measures use a gray-level spatial dependence matrix (i.e., gray-level co-occurrence matrix) to calculate texture values (Haralick et al. 1973), which indicates the probability that each pair of pixel values co-occur in a given direction and distance (Haralick et al. 1973; Mihran and Jain 1998). Some first-order texture measures are strongly correlated with second-order measures (i.e., mean, variance, and entropy; Wood et al. 2012); therefore, we selected second-order measures among these correlated variables because those measures considered the spatial relationships of pixels. We used the

following subset of texture measures: first-order (range) and second-order (mean, variance, contrast, entropy, second moment, and correlation).

All raw remote sensing variables, i.e., greenness indices, BI, and temperature values were extracted for the pixel that corresponds with each sample field point. Moreover, we calculated first-order texture measures using a 3×3 moving window size, i.e., the pixel values within a moving window were used to calculate a statistic that was assigned to the central pixel (Hall-Beyer 2007; Haralick et al. 1973). The second-order texture measures were calculated using the same moving window, but the pixel values were first translated into a gray-level co-occurrence matrix, which allowed us to consider the relationship among neighboring pixels (Hall-Beyer 2007; Haralick et al. 1973). All the texture measures were calculated separately for each of the raw remote sensing variables (the best green index, BI, and temperature). All the remote sensing variables were calculated using ENVI GIS (ENVI 2004).

Model building

We parameterized generalized linear models (GLMs) with remotely sensed independent variables, and with used (1) versus available (0) crevices by viscacha rats as response variables (binomially distributed). We used an information-theoretic approach described by Burnham and Anderson (2002) to model the data, based on the second-order Akaike Information Criterion (AIC). Akaike's information criterion corrected for small sample size (AICc) was calculated for each model. Models were compared with ΔAICc, which is the difference between the lowest AICc value (i.e., the best of suitable models) and AICc from all the other models. We considered an Akaike weight of a model (w_i), which determines the relative likelihood that the specific model is the best of the suite of all models. The w_i for a model is just exp ($−0.5×\Delta AIC_c$ score for that model) divided by the sum of these values across all models. We evaluated the support for predictor variables by summing w_i across all models that contained the parameter being considered (parameter likelihood; Burnham and Anderson 2002). Parameter estimates were calculated using

model-averaged parameter estimates based on w_i from all candidate models. To supplement parameter-likelihood evidence of important effects, we calculated 95 % confidence interval limits (CL) of parameter estimates.

We randomly divided occurrence data into training (70 %) and testing (30 %) datasets. The models were developed based on the training dataset ($N=130$), and then model performance was evaluated based on the testing dataset ($N=56$) with the area under the receiver operating characteristic curve (AUC). Model performance has a useful amount of discrimination with an AUC-value above 0.75 (Elith et al. 2006).

To identify collinearity, we used Spearman rank correlation, a non-parametric measure of statistical dependence, in order to remove correlated variables (Zar 1999). We built Spearman rank matrices and excluded variables when the coefficient r was >0.8 (Appendices 1, 2, 3, and 4). Then, we assessed the variance inflation factor (VIFs) on the full models from different sets, for any remaining collinearity and excluded variables with VIFs >5, which indicate collinearity between predictors (Heiberger and Holland 2004). To check for spatial-autocorrelation among sampling points, we fitted semivariograms with the Pearson residuals of the models containing all explanatory variables (Zuur et al. 2009). We did not find evidence of spatial dependence affecting the models.

The relationship between greenness indices and occurrence of the viscacha rat was assessed using univariate GLM. After selecting the green index that best fitted to the data, we fitted three partial models considering each raw index (i.e., the best green index, BI obtained from TC and temperature) with texture measures calculated from each index (first and second-order). To construct the global model, we took into account the variables from partial models with a confidence interval that excluded zero. From this global model, we constructed a habitat suitability map for the viscacha rat in the IPP using ENVI GIS (ENVI 2004) and Quantum GIS (Version 1.7.0 "Wroclaw"). The habitat suitability map predicted different habitat qualities for the species. All statistical analyses were conducted using R (2014).

Results

A total of 186 locations were recorded in the study area, of which 90 were used locations and 96 were available ones. The best green index to explain the occurrence of the viscacha rat was SATVI ($w_i=0.99$), followed by NDSVI ($w_i=0.01$), NDVI ($w_i<0.00$), SAVI ($w_i<0.00$), and GI ($w_i<0.00$).

When considering raw BI values and texture measures calculated from it, the best model included BI, second-order contrast, entropy, and variance (Table 1). This model had a good performance (AUC 0.82). The probability of occurrence of the viscacha rat decreased with increasing BI value and second-order contrast of BI (Table 4). Second-order entropy and

Table 1 Summary of model-selection results for models explaining the occurrence of the viscacha rat in relation to the Brightness Index (BI, no moving window analysis) and 2nd order texture measures calculated from BI in a 3×3 moving window. k is the number of estimated parameters. Models with $\Delta_i < 7$, univariate models and null model are shown and listed in decreasing order of importance

Model	k	AIC_c	Δ_i	w_i	R^2
BI+CON+ENT+VAR	5	131.72	0.00	0.64	0.49
BI+CONT+ENT	4	133.42	1.69	0.28	0.46
BI+CONT+VAR	4	136.23	4.51	0.07	0.44
BI	2	143.62	11.89	<0.00	0.36
ENT	2	181.92	50.20	<0.00	0.02
null	1	182.22	50.50	<0.00	0.00
CONT	2	183.54	51.82	<0.00	<0.00
VAR	2	184.24	52.52	<0.00	<0.00

BI sample-point pixel values

Second-order texture measure: *CON* contrast; *ENT* entropy; *VAR* variance

variance were not correlated with the occurrence of the viscacha rat (Table 4).

The best model for SATVI and its derived texture measures included raw values of SATVI and second-order contrast and entropy (Table 2). This model had a relatively good performance (AUC 0.72). The raw values of SATVI and second-order contrast were directly related to the probability of occurrence of the viscacha rat, contrarily to second-order entropy, which was inversely related (Table 4).

When considering raw temperature values and texture measures calculated from it, the raw values of temperature was the only variable included in the best model (Table 3). This model

Table 2 Summary of model-selection results for models explaining the occurrence of the viscacha rat in relation to the Soil Adjusted Total Vegetation Index (SATVI, no moving window analysis), 1st and 2nd order texture Vegetation Index (SATVI, no moving window analysis), 1st and 2nd order texture measures calculated from SATVI in a 3 × 3 moving window. k is the number of estimated parameters. Models with $\Delta_i < 7$, univariate models and null model are shown and listed in decreasing order of importance

Model	k	AIC_c	Δ_i	w_i	R^2
SATVI+CONT+ENT	4	115.73	0.00	0.63	0.57
SATVI+CONT+ENT+RG	5	117.84	2.11	0.22	0.53
SATVI+CONT	3	119.89	4.16	0.08	0.54
SATVI+CONT+RG	4	121.55	5.82	0.03	0.54
SATVI	2	122.52	6.79	0.02	0.50
CONT	2	180.94	65.21	<0.00	0.03
null	1	182.22	66.49	<0.00	<0.00
RG	2	184.20	68.48	<0.00	<0.00
ENT	2	184.25	68.52	<0.00	<0.00

SATVI sample-point pixel values

First-order measure: *RG* range; second-order measure: *CON* contrast, *ENT* entropy

had a good performance (AUC 0.78), but it has low variability explained (Table 3). The probability of occurrence of the viscacha rat decreased with increasing temperature (Table 4).

We included BI, SATVI, second-order contrast of BI, second-order contrast and entropy of SATVI in the selection of the best global model. Although the confidence interval for the temperature exclude zero, we did not include it in the global model because the univariate model with this variable has low variability explained (R^2=0.16). The best global model explained 60 % of the variability and had a good performance (AUC 0.74; Table 5). The equation of this model was used to map habitat suitability across the entire study area:

$$Y = 0.57 - 0.15 \, (\text{CON of BI}) + 37.41 \, (\text{SATVI})$$
$$+ 3.59 \, (\text{CON of SATVI}) - 2.10 \, (\text{ENT of SATVI})$$

where

BI	Brightness Index (sample-point pixel values)
SATVI	Soil Adjusted Total Vegetation Index (sample-point pixel values)
CON	Contrast (second-order texture measure)
ENT	Entropy (second-order texture measure)

This equation predicts the occurrence of the viscacha rat categorized into four probability classes (Fig. 3). Considering model-averaged parameter estimates, the raw values of SATVI and second-order contrast of SATVI were directly related to the probability of occurrence of the viscacha rat, in contrast to second-order contrast of BI and second-order entropy of SATVI which were inversely related (Table 6).

Table 3 Summary of model-selection results for models explaining the occurrence of the viscacha rat in relation to the temperature (T, no moving window analysis), 1st and 2nd order texture measures calculated from temperature in a 3 × 3 moving window. k is the number of estimated parameters. Models with Δ_i < 7, univariate models and null model are shown and listed in decreasing order of importance

Model	k	AIC$_c$	Δ_i	w_i	R^2
T	2	167.45	0.00	0.38	0.16
T+RG	3	167.63	0.18	0.35	0.18
T+ENT	3	169.32	1.88	0.15	0.16
T+RG+ENT	4	169.74	2.29	0.12	0.18
null	1	182.22	14.77	<0.00	0.00
RG	2	184.09	16.64	<0.00	<0.00
ENT	2	184.21	16.77	<0.00	<0.00

T sample-point pixel values

First-order measure: *RG* range; second-order measure: *ENT* entropy

Table 4 Parameter likelihoods, estimates (± SE) and 95 % confidence interval limits (CL) for explanatory variables describing the occurrence of the viscacha rat considering: BI (Brightness Index) and image texture of BI (a), SATVI (Soil Adjusted Total Vegetation Index) and image texture of SATVI (b), temperature and image texture of temperature (c). Explanatory variables with CL excluding zero are in italics

Explanatory variable	Parameter likelihood	Parameter estimate±SE	CL Lower	CL Upper
(a) BI and image texture of BI				
Intercept		*6.73±2.32*	*2.10*	*11.35*
BI	1.00	*−18.17±3.33*	*−24.76*	*−11.58*
Contrast	0.99	*−0.34±0.12*	*−0.58*	*−0.10*
Entropy	0.92	2.00±1.03	−0.04	4.04
Variance	0.71	0.47±0.25	−0.02	0.96
(b) SATVI and image texture of SATVI				
Intercept		0.19±0.89	−1.59	1.97
SATVI	1.00	*36.23±6.92*	*22.54*	*49.93*
Contrast	0.96	*3.08±1.20*	*0.68*	*5.49*
Entropy	0.86	*−2.26±1.00*	*−4.25*	*−0.27*
Range	0.27	2.72±18.69	−34.35	39.79
(c) Temperature and image texture of temperature				
Intercept		*29.96±7.85*	*14.39*	*45.53*
Temperature	1.00	*−0.76±0.20*	*−1.15*	*−0.37*
Range	0.47	−0.67±0.49	−1.65	0.31
Entropy	0.27	−0.09±0.50	−1.07	0.89

Discussion

This is the first study that evaluates the usefulness of different remotely sensed data as tools for predicting suitable habitats for a rock-dwelling species. We fitted partial models considering remote sensing data (i.e., raw indices and their derived texture measures) that provided information about habitat features important for the viscacha rat, such as rocky areas, vegetation, and temperature. Our findings showed strong relationships between occurrence of this species and raw index values (i.e., BI and SATVI) as well as with second-order texture measures calculated on BI and SATVI (i.e., contrast and entropy).

On the global model, SATVI was the best raw index to explain habitat selection of the viscacha rat, followed by second-order contrast and entropy of SATVI. Second-order contrast of BI, as opposed to BI only, made an important contribution to the model by capturing the heterogeneity of the substratum. This work adds evidence to support the usefulness of remote sensing data to identify suitable habitats for small-bodied rock-dwelling species in deserts.

BI showed an inverse relationship with the occurrence of the viscacha rat, i.e., used locations had lower values than available locations. BI provides information about reflectivity particularly generated by the soil. Martinelli (2009) and Gatica (2010) showed that BI is a useful index to determine

Table 5 Summary of model-selection results for global model explaining the occurrence of the viscacha rat. k is the number of estimated parameters. Models with $\Delta_i < 7$, univariate models and null model are shown and listed in decreasing order of importance

Model	k	AIC_c	Δ_i	w_i	R^2
CON (BI)+SATVI+CON (SATVI)+ENT (SATVI)	5	113.62	0.00	0.44	0.60
SATVI+CON (SATVI)+ENT (SATVI)	4	115.73	2.11	0.15	0.57
BI+ CON (BI)+SATVI+CON (SATVI)+ENT (SATVI)	6	115.77	2.15	0.15	0.60
CON (BI)+SATVI+CON (SATVI)	4	116.45	2.83	0.11	0.57
BI+SATVI+CON (SATVI)+ENT (SATVI)	5	117.85	4.23	0.05	0.57
BI+CON (BI)+SATVI+CON (SATVI)	5	118.61	4.99	0.04	0.57
SATVI+CON (SATVI)	3	119.89	6.27	0.02	0.53
SATVI	2	122.52	8.90	0.01	0.50
BI	2	143.62	30.00	<0.00	0.36
CONT (SATVI)	2	180.94	67.32	<0.00	0.03
null	1	182.22	68.60	<0.00	0.00
CONT (BI)	2	183.54	69.92	<0.00	0.01
ENT (SATVI)	2	184.25	70.63	<0.00	<0.00

BI Brightness Index (sample-point pixel values)

SATVI Soil Adjusted Total Vegetation Index (sample-point pixel values)

Second-order texture measure in a 3×3 moving window: *CON* contrast, *ENT* entropy

Table 6 Parameter likelihoods, estimates (± SE) and 95 % confidence interval limits (CL) for explanatory variables of the global model describing the occurrence of the viscacha rat. Explanatory variables with CL excluding zero are in italics

Explanatory variable	Parameter likelihood	Parameter estimate±SE	CL Lower	CL Upper
Intercept		0.57±0.81	−2.72	3.43
SATVI	*1.00*	*37.41±6.82*	*25.76*	*53.20*
CONT (SATVI)	*0.97*	*3.59±1.15*	*1.43*	*6.00*
ENT (SATVI)	*0.81*	*−2.10±0.98*	*−4.15*	*−0.25*
CONT (BI)	*0.76*	*−0.15±0.08*	*−0.33*	*−0.01*

BI Brightness Index (sample-point pixel values)

SATVI Soil Adjusted Total Vegetation Index (sample-point pixel values)

Second-order texture measure in a 3×3 moving window: *CON* contrast, *ENT* entropy

substratum heterogeneity in a desert. BI values are low because the rocky areas reflect less energy than areas with fine substrata (clay and sand soil; Riaza et al. 1994); high density of the rocky areas provides them with high thermal inertia (Campbell 2002). At microhabitat scale, the viscacha rat selected deep crevices which provide them with thermal stability and gradient, facilitating thermoregulation (Campos et al. 2013). Probably, the spatial resolution of temperature image make it difficult to discern fine resolution patterns of viscacha

Fig. 3 Probability area for occurrence of the viscacha rat categorized into four probability classes according to the best global model
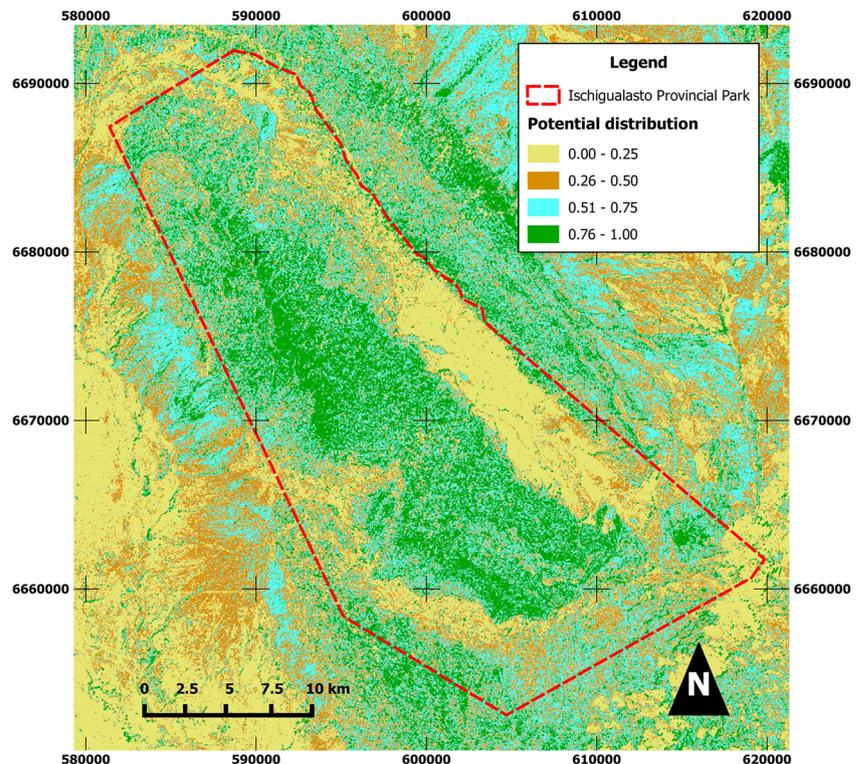
rat occurrence, so the variability explained by univariate model of temperature was very low. Moreover, our results showed that SATVI was the best greenness index; SATVI is sensitive to green and senescent vegetation because it uses the short-wave infrared band reflectance (bands 5 and 7 in the TM sensor) and furthermore includes the effect of bare soil factor (Marsett et al. 2006), an important variable to be considered in arid environments. This greenness index was the best predictor of cover vegetation in the Monte Desert (Goirán et al. 2012). The positive relationship between this index and occurrence of the viscacha rat supports the idea proposed by Mares (1997) that rocky habitats are able to maintain more complex vegetation than much of the surrounding desert. The plants associated with rocks are often greener for longer periods due to increased water availability afforded by the rocks; they offer food, shade and shelter, largely contributing to habitat complexity, suitability and microclimate (Mares 1997).

Image texture measures are useful for characterizing differences in habitat heterogeneity that determine spatial patterns of species richness across the landscape. This approach can act as surrogate for habitat structure and represents a cost-effective way of mapping habitat heterogeneity besides being a promising tool for predicting patterns of species richness (St-Louis et al. 2006, 2009; Wood et al. 2012, 2013). Second-order contrast and entropy of indices were included in the best partial models and global model. Second-order contrast is a measure of spatial frequency, i.e., the difference between the highest and the lowest values of a contiguous set of pixels (Baraldi and Parmiggiani 1995). This measure gathers clusters starting from strongly contrasted areas; the negative relationship with the occurrence of the viscacha rat showed that large regions of low and medium contrast image, i.e., rocky habitats, are associated with the same background cluster and are strongly separated from the values of high contrast areas, i.e., available locations. The positive relationship between the occurrences of the viscacha rat with contrast texture of SATVI indicated a high contrast in vegetation for rocky habitats. Wood et al. (2012) found second-order contrast to be highly related to foliage-height diversity among habitats; hence, these authors recommend using this measure to characterize vegetation structure patterns. Another measure recommended for mapping wildlife habitats across broad spatial extents (Wood et al. 2012) is entropy, a measure of disorder in the image (Baraldi and Parmiggiani 1995). The occurrence of the viscacha rat had a negative relationship with second-order entropy of SATVI, which showed that vegetation in rocky habitats did not have a random distribution but rather had clumped distribution in comparison with available habitats, as proposed by Mares (1997).

The best global model identified the habitats with different probability of occurrence of the viscacha rat. This model included raw index and texture measures, which explained above 60 % of the variability of viscacha rat occurrence. The habitat preferences identified in our models are consistent

with the results of field studies of use of landscape by the viscacha rat. The substratum of rocky habitats was well differentiated by the second-order contrast of BI, instead of BI only. Our results are consistent with previous studies, which demonstrated that image texture calculated from remotely sensed data is an effective tool for measuring habitats across broad spatial extents (St-Louis et al. 2006, 2009; Bellis et al. 2008; Wood et al. 2012, 2013). Furthermore, crevices with high vegetation cover could be estimated through SATVI, a greenness index sensitive to green and senescent vegetation, and its second-order contrast and entropy.

The range of current resource-use strategies are survivors of long-term adaptation (Fortin et al. 2008). Habitat specialist species have rigid habitat requirements so they are markedly vulnerable to habitat alterations (Devictor et al. 2008) and are prone to extinction (Pimm and Askins 1995; Pitman et al. 2002; Thomas et al. 2004). Protection strategies require information on predictors of habitat quality and their spatially explicit depiction; however, continuous spatial measurements of habitat quality can be difficult to acquire across broad spatial extents. Our findings will contribute to identify suitable habitats for rock-dwelling mammals through remotely sensed data, because raw indices and texture measures were able to detect important aspects of the landscape for the viscacha rat. Our results contribute to conservation efforts of habitat specialist species by using good predictors of habitat quality for this species. Managers could use predictive models considering the variables here suggested to identify patterns of occurrence of other rock-dwelling species.

References

Austin MP, Nicholls AO, Doherty MD, Meyers JA (1994) Determining species response functions to an environmental gradient by means of a beta-function. J Veg Sci 5:215–228

Baraldi A, Parmiggiani F (1995) An investigation of textural characteristics associated with gray level co-occurrence matrix statistical parameters. IEEE Trans Geosci Remote Sens 33:293–304

Bellis LM, Pidgeon AM, Radeloff VC, St-Louis V, Navarro JL, Martella MB (2008) Modeling habitat suitability for greater rheas based on satellite image texture. Ecol Appl 18:1956–1966

Bolstad PV, Lillesand TM (1992) Improved classification of forest vegetation in northern Wisconsin through a rule-based combination of soils, terrain, and landsat thematic mapper data. For Sci 38:5–20

Boyce MS, Vernier PR, Scott EN, Schmiegelow FKA (2002) Evaluating resource selection functions. Ecol Model 157:281–300

Bradley BA, Olsson AD, Wang O, Dickson BG, Pelech L, Sesnie SE, Zachmann LJ (2012) Species detection vs. habitat suitability: are we biasing habitat suitability models with remotely sensed data? Ecol Model 244:57–64

Brown DG (1994) Predicting vegetation types at treeline using topography and biophysical disturbance variables. J Veg Sci 5:642–656

Burnham KP, Anderson DR (2002) Model selection and multimodel inference. A practical information—theoretic approach. Springer, New York

Campbell JB (2002) Introduction to remote sensing. The Guilford Press, New York

Campos VE (2012) Biología de Octomys mimax (Rodentia: Octodontidae): selección de hábitat y conservación en el Monte árido de San Juan. Dissertation, Universidad Nacional de Córdoba; Argentina

Campos VE, Giannoni SM (2013) Habitat selection by the viscacha rat (Octomys mimax, Rodentia: Octodontidae) in a spatially heterogeneous landscape. Mamm. doi:10.1515/mammalia-2013-0078

Campos VE, Andino N, Cappa F, Reus L, Giannoni S (2013) Microhabitat selection by Octomys mimax (Rodentia: Octodontidae) in the Monte Desert is affected by attributes and thermal properties of crevices. Rev Chil Hist Nat 86:315–324

Card D (1982) Using know map category marginal frequencies to improve estimates of thematic map accuracy. Photogramm Eng Remote Sens 48:431–439

Crist CP, Cicone RC (1984) Application of the tasseled cap concept to simulate thematic mapper data. Photogramm Eng 50:343–352

Devictor V, Julliard R, Jiguet F (2008) Distribution of specialist and generalist species along spatial gradients of habitat disturbance and fragmentation. Oikos 117:507–514

Ebensperger LA, Sobrero R, Campos V, Giannoni SM (2008) Activity, ranges areas, and nesting patterns in the viscacha rat, Octomys mimax: implications for its social organization. J Arid Environ 72:1174–1183

Elith J, Graham CH, Anderson RP, Dudík M, Ferrier S, Guisan A, Hijmans RJ, Huettmann F, Leathwick JR, Lehmann A, Li J, Lohmann LG, Loiselle BA, Manion G, Moritz C, Nakamura M, Nakazawa Y, Overton JMC, Townsend Peterson A, Philli SJ (2006) Novel methods improve prediction of species'distribution from occurrence data. Ecography 29:129–151

ENVI (2004) Environment for visualizing images. Version 4.1. Research Systems, Boulder, Colorado

Estes LD, Okin GS, Mwangi AG, Shugart HH (2008) Habitat selection by a rare forest antelope: a multi-scale approach combining field data and imagery from three sensors. Remote Sens Environ 112:2033–2050

Fortin D, Morris DW, McLoughlin PD (2008) Habitat selection and the evolution of specialist in heterogeneous environments. Israel J Ecol Evol 54:311–328

Gatica MG (2010) Estudio del estado y cambio temporal de la cobertura vegetal usando teledetección, sistemas de información geográfica y técnicas cuantitativas de ecología de paisajes en un sitio del Monte Central, San Juan (Argentina). Dissertation, Universidad Nacional de San Juan, Argentina

Ge S, Carruthers R, Gong P, Herrera A (2006) Texture analysis for mapping Tamarix parviflora using aerial photographs along the cache creek, California. Environ Monit Assess 114:65–83

Goirán SB, Aranibar JN, Gomez ML (2012) Heterogeneous spatial distribution of traditional livestock settlements and their effects on vegetation cover in arid groundwater coupled ecosystems in the Monte Desert (Argentina). J Arid Environ 87:188–197

Gottschalk TK, Huettmann F, Ehlers M (2005) Thirty years of analyzing and modeling avian habitat relationships using satellite imagery data: a review. Int J Remote Sens 26:2631–2656

Gould W (2000) Remote sensing of vegetation, plant species richness, and regional biodiversity hotspots. Ecol Appl 10:1861–1870

Hall-Beyer M (2007) The GLCM tutorial home page. Current Version 2.10

Haralick RM, Shanmugam K, Dinstein I (1973) Textural features for image classification. IEEE Trans Syst Man Cybern SMC-3:610–621

Heiberger RM, Holland B (2004) Statistical analysis and data display: an intermediate course with examples in S-plus, R, and SAS. Springer Texts in Statistics, New York

Herfindal I, Solberg EJ, S ther BE, Høgda KA, Andersen R (2006) Environmental phenology and geographical gradients in moose body mass. Oecologia 150:213–224

Huete AR (1988) A soil-adjusted vegetation index (SAVI). Remote Sens Environ 25:295–309

Johnson CJ, Nielsen SE, Merrill EH, McDonald TL, Boyce MS (2006) Resource selection functions based on use-availability data: theoretical motivation and evaluation methods. J Wildl Manag 70:347–357

Kauth RJ and Thomas GS (1976) The tasseled cap- a graphic description of the spectral temporal development of agricultural crops as seen in Landsat. Proc Symp Machine Process Remotely Sensed Data 41–51

Labraga JC, Villalba R (2009) Climate in the Monte desert: past trends, present conditions, and future projections. J Arid Environ 73:154–163

Labrandero JL (1978) Aplicación de métodos digitales al reconocimiento de suelos mediante sensores remotos. Thesis Universidad Autónoma de Madrid, España

Mares MA (1997) The geobiological interface: granitic outcrops as a selective force in mammalian evolution. JR Soc West Aust 80:131–139

Márquez J, Martínez Carretero E, Dalmasso A, Pastrán G, Ortiz G (2005) Las áreas protegidas de la provincia de San Juan (Argentina) II. La vegetación del Parque Provincial de Ischigualasto. Multequina. Lat Am J Nat Resour 14:1–27

Marsett RC, Qi J, Heilman P, Biedenbender SH, Watson MC, Amer S, Weltz M, Goodrich D, Marsett R (2006) Remote sensing for grassland management in the arid southwest. Rangeland Ecol Manag 59:530–540

Martinelli M (2009) Caracterización de la degradación de tierras en sistemas productivos de zonas áridas, en Valle Fértil, Noreste de San Juan, Argentina. Identificación de indicadores. Dissertation, Universidad Nacional de Río Cuarto, Argentina

Mihran T, Jain AK (1998) Texture analysis. In Chen CH, Pau LF, Wang PSP (eds.) The handbook of pattern recognition and computer vision. Word Scientific Publishing Co, pp 207–248

Nagendra H (2001) Using remote sensing to assess biodiversity. Int J Remote Sens 22:2377–2400

Nutt KJ (2007) Socioecology of rock-dwelling rodents. In: Wolf JO, Sherman PW (eds) Rodent societies: an ecological and evolutionary perspective. Chicago University Press, Chicago and London, pp 193–402

Olofsson P, Foody GM, Stehman SV, Woodcock CE (2013) Making better use of accuracy data in land change studies: estimating accuracy and area and quantifying uncertainty using stratified estimation. Remote Sens Environ 129:122–131

Osborne PE, Alonso JC, Bryant RG (2001) Modelling landscape-scale habitat use using GIS and remote sensing: a case study with great bustards. J Appl Ecol 38:458–471

Pettorelli N, Olav Vik J, Mysterud A, Gaillard JM, Tucker CJ, Stenseth NC (2005) Using the satellite-derived NDVI to assess ecological responses to environmental change. Trends Ecol Evol 20:503–510

Pimm SL, Askins RA (1995) Forest losses predict bird extinctions in eastern North-America. Proc Natl Acad Sci U S A 92:9343–9347

Pitman NCA, Jorgensen PM, Williams RSR, Leon-Yanez S, Valencia R (2002) Extinction-rate estimates for a modern neotropical flora. Conserv Biol 16:1427–1431

Quantum GIS Version 1.7.0 "Wroclaw" Development Team, 2010. QGIS Geographic Information System. Open Source Geospatial Foundation Project. http://qgis.osgeo.org/

R Core Team (2014) A language and environment for statistical computing. R Foundation for Statistical Computing, Vienna, Austria. URL http://www.R-project.org/

Riaza A, Escuder J, Villar P, Alfageme SM (1994) Reflectancia espectral en el visible e infrarrojo cercano (400–2500 nm) de distintas litologías en un conjunto ígneo y metamórfico (Salamanca, España): aplicaciones en cartografía geológica. Rev Soc Geol Esp 7:7–20

Rogers DJ, Randolph SE, Snow RW, Hay SI (2002) Satellite imagery in the study and forecast of malaria. Nature 415:710–715

Schott JR, Volchok WJ (1985) Thematic mapper thermal infrared calibration. Photogramm Eng Remote Sens 51:1351–1357

St-Louis V, Pidgeon AM, Radeloff VC, Hawbaker TJ, Clayton MK (2006) Image texture in high-resolution remote sensing images as predictor of bird species richness. Remote Sens Environ 105:299–312

St-Louis V, Pidgeon AM, Clayton MK, Locke BA, Bash D, Radeloff VC (2009) Satellite image texture and a vegetation index predict avian biodiversity in the Chihuahuan desert of New Mexico. Ecography 32:468–480

Thomas CD, Williams SE, Cameron A, Green RE, Bakkenes M, Beaumont LJ, Collingham YC, Erasmus BFN, de Siqueira MF, Grainger A, Hannah L, Hughes L, Huntley B, van Jaarsveld AS, Midgley GF, Miles L, Ortega-Huerta MA, Peterson AT, Phillips OL (2004) Biodiversity conservation – uncertainty in predictions of extinction risk – effects of changes in climate and land use – climate change and extinction risk – reply. Nature 430

Traba J, Acebes P, Campos VE, Giannoni SM (2010) Habitat selection by two sympatric rodent species in the Monte desert Argentina. First data for Eligmodontia moreni and Octomys mimax. J Arid Environ 74:179–185

Turner W, Spector S, Gardiner N, Fladeland M, Sterling E, Steininger M (2003) Remote sensing for biodiversity science and conservation. Trends Ecol Evol 18:306–314

Walker RS, Novaro AJ, Branch LC (2003) Effects of patch attributes, barriers, and distance between patches on the distribution of a rock-dwelling rodent (Lagidium viscacia). Landsc Ecol 18:185–192

Willems EP, Hill RA (2009) A critical assessment of two species distribution models: a case study of the vervet monkey (Cercopithecus aethiops). J Biogeogr 36:2300–2312

Wood EM, Pidgeon AM, Radeloff VC, Keules NS (2012) Image texture as a remotely sensed measure of vegetation structure. Remote Sens Environ 121:516–526

Wood EM, Pidgeon AM, Radeloff VC, Keuler NS (2013) Image texture predicts avian density and species richness. Plos One 8. doi: 10.1371/journal.pone.0063211

Zar JH (1999) Biostatistical analysis. Prentice-Hall, USA

Zuur A, Ieno EN, Walker N, Saveliev AA, Smith GM (2009) Mixed effects models and extensions in ecology with R. Springer, New York